HOKKAIDO UNIVERSITY

| | |
|---|---|
| Title | Alkali Leaching of Ni-Al Alloy Microchannel Lining Layers |
| Author(s) | Saitoh, Yuhsuke; Ohmi, Tatsuya; Sakairi, Masatoshi et al. |
| Citation | 実験力学, 11(Special Issue), s276-s279<br>https://doi.org/10.11395/jjsem.11.s276 |
| Issue Date | 2011 |
| Doc URL | https://hdl.handle.net/2115/74642 |
| Rights | 著作権は日本実験力学会にある。利用は著作権の範囲内に限られる。 |
| Type | journal article |
| File Information | J.JSEM 11. s276.pdf |

Hokkaido University Collection of Scholarly and Academic Papers : HUSCAP

Journal of JSEM, Vol.11, Special Issue (2011) SS276-SS279
Copyright © 2011 JSEM

# Alkali Leaching of Ni-Al Alloy Microchannel Lining Layers

Yuhsuke SAITOH[1], Tatsuya OHMI[2], Masatoshi SAKAIRI[2] and Manabu IGUCHI[2]

[1] Graduate School of Engineering, Hokkaido University, Sapporo 060-8628, Japan
[2] Faculty of Engineering, Hokkaido University, Sapporo 060-8628, Japan

(*Received 11 January 2011; received in revised form 31 May 2011; accepted 5 June 2011*)

**Abstract**
We investigate alkali leaching of Ni-Al alloy microchannel lining layers to produce a metallic microreactor for high-temperature catalytic reactions. The microchannels and the lining layers were produced by a powder-metallurgical microchanneling process with Ni powder and Al wires. We explored the conditions for the process to produce an $Al_3Ni$ or $Al_3Ni_2$ lining layer. The Al concentration of the lining layers was successfully decreased by alkali leaching.

**Key words**
Microchannel, Powder Metallurgy, Alkali Leaching, Intermetallic Compound, Raney-Nickel Catalyst

## 1. Introduction

The improvement of the catalyst technology is one of the possible solutions to the environmental problems. The challenges of the catalyst technology are exploring new low-cost catalyst materials and developing excellent reactor configuration. A metallic microreactor has a microchannel structure with high specific surface area and good heat conductivity. Therefore, the metallic microreactor is suitable for catalytic reactions.

Some of the authors investigated a powder-metallurgical microchanneling process in previous studies [1-4]. The concept for the process was based on microscopic infiltration and diffusion phenomena which often occur during liquid phase sintering of a mixture of powder metals with different melting points. They used the metal with higher melting point as a body metal, which is to compose the device body, and the other as a sacrificial-core metal, which is to flow out and give the shape of the microchannel. They found that a porous thick film of intermetallic compounds formed as a lining layer when nickel was used as the body metal and aluminum as the sacrificial-core metal. [4] Figure 1 shows an example of the structure of the porous thick film. This specimen was sintered at 1473 K. The lining layer in this specimen consisted of NiAl phase. Figure 2 depicts a Ni-Al binary alloy phase diagram [5]. The solid phase in equilibrium with Al-rich liquid changes depending on the temperature: $Al_3Ni$, $Al_3Ni_2$ and NiAl. The actual phase of the lining layer changes with the sintering temperature and duration.

Some studies have been carried out to give catalytic activity to Ni-Al intermetallic compounds. For example, alkali-leached $Ni_3Al$ powder exhibits catalytic activity for hydrogen production from methanol and methane. [6-10] A mixture of $Al_3Ni$ and $Al_3Ni_2$ is well known as a precursor alloy for the Raney-Ni catalysts [11-13]. Consequently, if alkali leaching process can provide catalytic activity to the Ni-Al alloy microchannel lining layer, low-cost microreactor for catalytic reactions can be produced. In this research, heat treatment conditions which make $Al_3Ni$ or $Al_3Ni_2$ lining layer are explored, and then, changes of the structure and composition of the lining layer by alkali leaching are investigated.

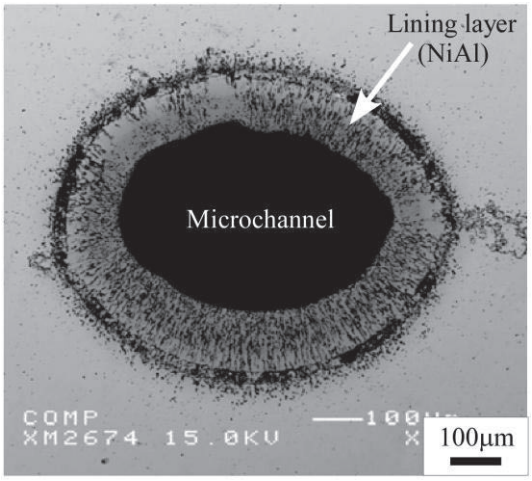


Fig. 1 Microporous structure of the NiAl lining layer [4]

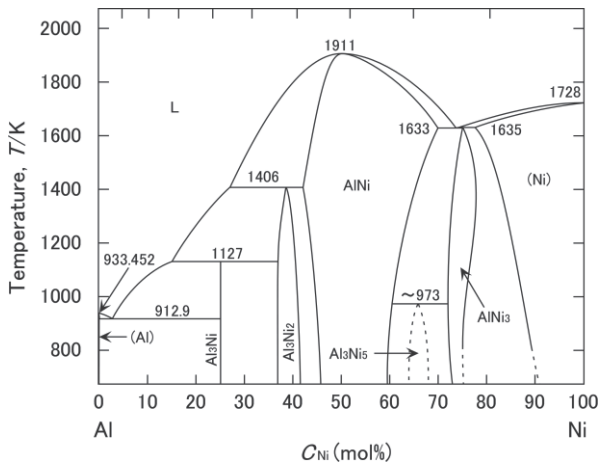


Fig. 2 Ni-Al binary alloy phase diagram [5]

## 2. Experimental Procedure

### 2.1 Preparation of green compacts

We used 13.9 g of nickel powder and three aluminum wires as the body-metal powder and the sacrificial cores, respectively. The average diameter of the nickel powder was 5 μm. The sacrificial cores were 500 μm in diameter and 10 mm in length. The nickel powder containing the

sacrificial cores was cold-pressed into a cylindrical green compact in a stainless steel mold using a unidirectional pressure of 460 MPa. The shape of the resulted compact specimen was a columnar 20 mm in diameter and 5 mm in height. The initial cross section of the aluminum wire was round. However, the sacrificial core was distorted into an oblate figure by unidirectional pressing, and the resulted microchannel and lining layer often inherited the shape of the sacrificial core as presented in Fig. 1.

### 2.2 Heat treatment conditions

The green compacts were sintered in an argon gas atmosphere. Figure 3 illustrates the time-temperature patterns during sintering heat treatment. The broken line in Fig. 3 indicates the standard pattern used for Ni-Al microchanneling experiments in the previous study [4].

In our experiments, we examined six patterns in order to control the composition of the lining layer. In the cases of the time-temperature patterns A, B and C, the specimens were quenched after sintering. The quenching was carried out by dipping in a molten Wood's metal. The cooling rate during quenching was about 160 K/s. During the microchannel formation in this process, the inner surface of the lining layer is in contact with the Al-rich liquid originating in the sacrificial-core metal. According to the phase diagram shown in Fig. 2, each solid phase in equilibrium with the Al-rich liquid is NiAl at 1473 K; $Al_3Ni_2$ at 1273 K and 1173 K; and $Al_3Ni$ at 1073 K. After the Al-rich liquid dries up, the Al concentration of the lining layer decreases by solid-state diffusion of Al. Therefore, the constituent phase of the inner surface of the lining layer depends on the heat treatment temperature and time.

### 2.3 Alkali leaching treatment

The specimen after sintering was cut to thickness of 5 mm. The microchannel penetrated the specimen in the thickness direction. The specimen after cutting was dipped in a NaOH aqueous solution for 86.4 ks in order to leach aluminum. The concentration of the NaOH aqueous solution was 7 kmol/m$^3$. In addition, another specimen heat-treated with pattern B' was cut along the microchannel, and dipped in the NaOH aqueous solution for 7.2 ks.

The structures of the specimens before and after alkali leaching were observed by SEM. The composition near the microchannel was analyzed by EPMA.

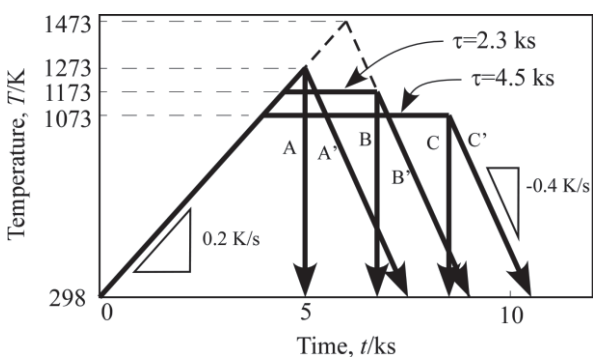


Fig. 3 Time-temperature patterns for sintering heat treatments. τ: holding time

## 3. Results

Table 1 Influence of the heat-treatment condition on the microchanneling behavior and the constituent phase of the lining layer

| Specimen | Microchannel formation | Constituent phase of lining layer |
|---|---|---|
| A | △ | $Al_3Ni_2$ |
| A' | ○ | $Al_3Ni_2$ |
| B | ○ | $Al_3Ni_2$ |
| B' | ○ | $Al_3Ni_2$ |
| C | △ | $Al_3Ni$ and $Al_3Ni_2$ |
| C' | ○ | $Al_3Ni$ and $Al_3Ni_2$ |

○: Opened
△: Partially-closed

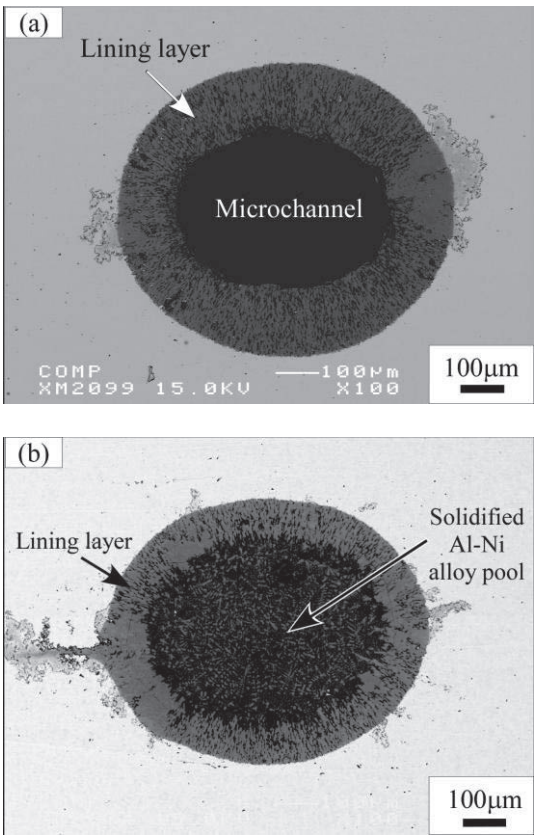


Fig. 4 Back-scattered electron images near the sites initially occupied by the sacrificial cores. (a) Specimen B', (b) specimen A

### 3.1 Formation of the microchannel

Table 1 lists the microchanneling behaviors and the constituent phases of the lining layers observed after sintering. Figure 4 shows the back-scattered electron (BSE) images of two kinds of typical structures near the sites initially occupied by the sacrificial cores. In Fig. 4 (a), the microchannel and lining layer had already formed. Similar structures formed in specimens A', B and C'. On the other hand, in Fig. 4 (b), the sacrificial core still remained at the original site. The Al, $Al_3Ni$ and $Al_3Ni_2$ phases were detected in the solidified Al-Ni alloy pool region, and the lining layer consisted of the $Al_3Ni_2$ phase. However, a microchannel-like cavity was observed on another cut plane. It means the specimen was in midstream of microchanneling before quenching. Similar structure formed in specimen C.

### 3.2 Change of the structure and composition of the lining layer by alkali leaching

Figure 5 shows the BSE images of the lining layer in specimen B' before and after alkali leaching. EPMA results showed that the average Al concentration of the lining layer was 61.2 mol% before alkali leaching. According to the phase diagram, the corresponding phase was $Al_3Ni_2$. The average composition of the lining layer was changed to Ni-29.6mol%Al-27.7mol%O by alkali leaching. This result indicated that the lining layer was dealloyed and oxidized by alkali leaching. In general, Raney-Ni catalysts are very easy to oxidize because of its huge specific surface area. For this reason, Raney-Ni catalysts are preserved in water or ethanol. The lining layer was probably oxidized during the structure observation after alkali leaching.

Figure 6 shows the BSE images of the lining layer in specimen A after alkali leaching. Before alkali leaching, the

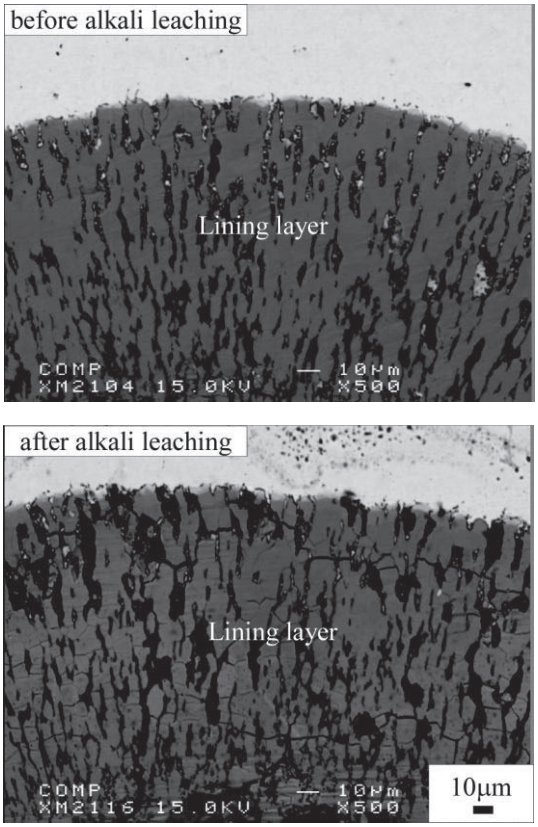


Fig. 5 Influence of alkali leaching on the lining-layer structure in specimen B'

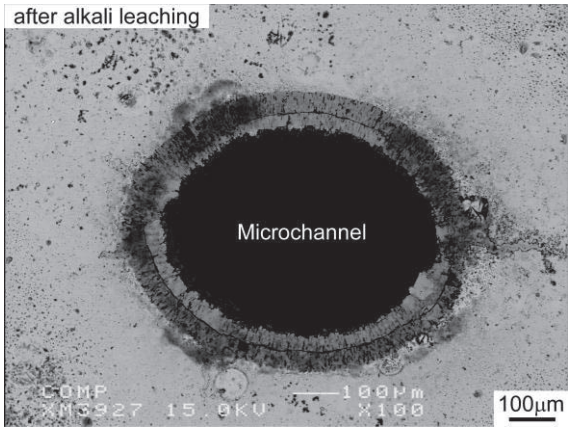


Fig. 6 Dissolution of the solidified Al-Ni alloy pool by alkali leaching for specimen A

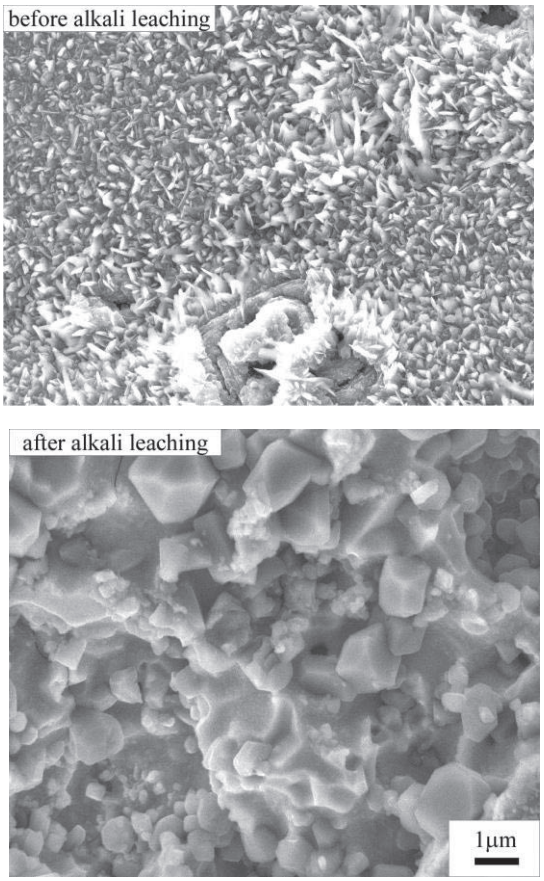


Fig. 7 Effect of alkali leaching on the structure of the inner-wall surface of the microchannel in specimen B'

microchannel was blocked by the solidified Al-Ni alloy pool as shown in Fig. 4 (b). However, this structure was dissolved during alkali leaching. This suggests that the microchannel can be completed by alkali leaching even if it is not fully open just after sintering. The average composition of the alkali-leached lining layer was Ni-27.8mol%Al-33.1mol%O.

Figure 7 presents the FE-SEM images of the inner-wall surface of the microchannel in specimen B' before and after alkali leaching. Needle-like structures was observed on the inner wall of the microchannel before alkali leaching. This structure is similar to the $Al_2O_3$ scale produced by high-temperature oxidation of NiAl [14]. It is speculated that the microchannel lining layer was oxidized by air slightly remained in the compact specimen. In the specimen after alkali leaching, faceted asperities of about dozens nm in diameter had formed on the inner wall of the microchannel. Detailed analysis on this structure will be a future subject. In any case, the alumina scale is easily dissolved in the sodium hydroxide solution. Instead, room-temperature oxidation after leaching should be prevented.

## 4. Conclusions

The heat treatment condition to make a microchannel lining layer consisting of $Al_3Ni$ or $Al_3Ni_2$ was explored. The effect of alkali leaching on the structure and composition of the lining layer was investigated. The results obtained are summarized as follows.

(1) The microchannel was in midstream of forming in the specimens quenched at 1273 K just after getting to the temperature and quenched at 1073 K after 4.5 ks-holding.

(2) The lining layers in the specimens quenched and furnace-cooled at 1073 K after 4.5 ks-holding consisted of the $Al_3Ni$ and $Al_3Ni_2$ phases. The lining layers in the other specimens consisted of the $Al_3Ni_2$ phase.

(3) The solidified Al-Ni alloy pool blocking the microchannel was dissolved by alkali leaching.

(4) The Al concentration of the Ni-Al lining layer was decreased by alkali leaching. The structure of the inner-wall surface of the microchannel was also changed to form submicron faceted asperities.

## References


[1] Ohmi, T., Kodama, T. and Iguchi, M.: Formation Mechanism of Microchannels and Lining Layers in Sintered Iron Powder Compacts with Copper Sacrificial Cores, *Mater. Trans.*, **50** (2009), 2891-2896.

[2] Ohmi, T., Takatoo, M., Iguchi, M., Matsuura, K. and Kudoh, M.: Powder-Metallurgical Process for Producing Metallic Microchannel Devices, *Mater. Trans.*, **47** (2006), 2137-2142.

[3] Ohmi, T., Takatoo, M. and Iguchi, M.: Powder-Metalugical Free-Form Microchanneling Process for Producing Metallic Microreactors, *J. JSEM*, **9** (2009), 125-129.

[4] Ohmi, T., Hayashi, N. and Iguchi, M.: Formation of Porous Intermetallic Thick Film by Ni-Al Microscopic Reactive Infiltration, *Mater. Trans.*, **49** (2008), 2723-2727.

[5] Okamoto, H.: Binary Alloy Phase Diagrams (2nd. ed., Plus Updates), *Materials Park*, (1996) (CD-ROM).

[6] Qi, C., Amphlett, C.J. and Pepply, A.B.: Hydrogen Production by methanol reforming on NiAl layered double hydroxide derived catalyst: Effect of the pretreatment of the catalyst, *Int. J. Hydrogen Energy*, (2007), 5098-5102.

[7] Xu, Y., Kameoka, S., Kishida, K., Demura, M., Tsai, P.A. and Hirano, T.: Catalytic Properties of $Ni_3Al$ Intermetallics for Methanol Decomposition, *Mater. Trans.*, **45** (2005), 3177-3179.

[8] Xu, Y., Kameoka, S., Kishida, K., Demura, M., Tsai, P.A. and Hirano, T.: Catalytic properties of alkali-leached $Ni_3Al$ for hydrogen production from methanol, *Intermetallics,* **13** (2005), 151-155.

[9] Xu, Y., Demura, M. and Hirano, T.: Effect of alkali leaching on the surface structure of $Ni_3Al$ catalyst, *Applied Surface Science*, **254** (2008), 5413-5420.

[10] Ma, Y., Xu, Y., Demura, M., Chun, H.D., Xie, G. and Hirano, T.: Catalytic activity of atomized $Ni_3Al$ powder for hydrogen generation by methane steam reforming, *Catalysis Letters*, **112** (2006), 31-36.

[11] Zou, J.J., Zhang, X., Kong, J. and Wang, L.: Hydrogenation of Dicyclopentadiene over amorphous nickel alloy catalyst SRNA-4, *Fuel*, **87** (2008), 3655-3659.

[12] Lei, H., Song, Z., Tan, D., Bao, X., Mu, X., Zong, B. and Min, E.: Preparation of novel Raney-Ni catalysts and characterization by XRD, SEM and XPS, *Applied Catalysis A: General*, **214** (2001), 69-76.

[13] Kudo, K. and Komatsu, K.: Selective formation of methane in reduction of $CO_2$ with water by Raney alloy catalyst, *J. Molecular Catalysis A: Chemical*, **145** (1999), 257-264.

[14] Liu, G., Li, M., Zhu, M. and Zhou, Y.: Transient of alumina oxide scale on B-NiAl coated on M38G alloy at 950˚C, *Intermetallics*, **15** (2007), 1285-1290.